

# Lake-Bottom Deformation Special Equipment Measurement Methods and Practice of Mining Under Weishan Lake

**Yuanzhong Luan \***, **Liyuan Weng**, **Yanhe Ma**, **Hengxuan Luan**

*Shandong University of Science and Technology, College of Geomatics,  
Qingdao Shandong 266590, China*

*\*Corresponding author: Geomatic College, Shandong University of Science and  
Technology, Qingdao 266590, China; e-mail: [lyzsdust@163.com](mailto:lyzsdust@163.com)*

## ABSTRACT

Aiming at the problem of lake-bottom deformation measurement under Weishan Lake, "the inverted vertical line measuring points method" and "the underwater measuring points with specially-made measuring rod method" are designed respectively for deep water and shallow water. Because these two devices need to use GPS-RTK technology, the static GPS and fourth-order leveling experiments are carried out in mining area to determine the relationship model between the distance between base and rover station and GPS-RTK plane and elevation measurement accuracy. This technology is applied for lake-bottom deformation of a mine in Shandong Province. The observation results show that the method has high precision, which provides a new and reliable method for under water deformation measurement. Based on the gray system theory, a real-time GM (1,1) 6-D real-time prediction model is established to reflect the deformation of the lake bottom. The real-time dynamic and high-precision prediction of lake-bottom deformation is realized, which provides a new method of deformation monitoring and prediction for realizing safety mining of coal seam under water.

**KEYWORDS:** GPS-RTK; specially-made measuring rod; inverted vertical line; lake-bottom deformation measurement; measuring accuracy

## INTRODUCTION

Mining will lead to different degree of settlement on the ground and buildings, which not only affecting the normally use and have a negative impact on people's lives and property, but also cause the loss of underground resources. Therefore, the analysis and prediction of mine deformation is getting more and more domestic and foreign experts' attention<sup>[1,2]</sup>.

Regular settlement measurement of the mining area can correctly predict the mining subsidence; take timely preventive and remedial measures to ensure the safety of mine production<sup>[3]</sup>. At present, the gray forecasting model have been widely used in a variety of forecasting problems because of its advantages of less modeling information, simpler operation and higher modeling accuracy. Liu Hechun and Guo Qiu<sup>[4]</sup> constructed the GM(1,1) subsidence prediction based on the gray theory and predicted the surface subsidence of the mining area; Song Shijie and Zhao Xiaoguang<sup>[5]</sup> researched

the relationship between the maximum surface subsidence coefficient and the influencing factors using the grey relational analysis method; Fan Hongdong and Yang Junkai <sup>[6]</sup> established the prediction function based on the grey verhulst model to analysis the development regularity of mining subsidence.

In addition, with the urgent need for the coal resources development, the “under-three mining” technology (under water, under buildings and under railway) developed rapidly <sup>[7-11]</sup>. Underwater exploitation refers to safe mining in the condition that water exists in the ground surface or the coal seam. The application of GPS-RTK technology in underwater terrain such as ocean, lake and river becomes more and more because the higher positioning accuracy, farther data transmission distance and higher reliability <sup>[12-17]</sup>. At present, there are more than 10 coal mines under the Weishan Lake. The difficulties of the lake bottom deformation measurement are the production and embedding of the rock movement measuring points and the lake bottom deformation measurement method. In this paper, “the inverted vertical line measuring points method” and “the underwater measuring points with specially-made measuring rod method” are put forward, also using GPS-RTK technology for plane and elevation measurement of the lake area. At the same time, static GPS plan measurement and leveling elevation measurement were carried out and compared with GPS-RTK measurement data.

## SPECIAL MEASUREMENT DEVICES AND MEASUREMENT METHOD

### Special measurement devices

“The inverted vertical line measuring points method” is designed according to the deformation measurement of lake’s bottom under deep water. The design structure is shown in Fig.1, which composed of inverted vertical line, protection tube and buoyancy device. The principle of this method is the top and bottom of inverted vertical line has equal two-dimensional coordinates when this device is stationary. The protection tube keeps the inverted vertical line stay in a state of still water, avoiding the influence of other objects. Buoyancy device is composed of a float and a water tank, to make sure the inverted vertical line stay in a vertical plane.

“The underwater measuring points with specially-made measuring rod method” is designed according to the deformation measurement of lake’s bottom under shallow water. The structure of the specially-made measuring rod is shown in Fig.2, The design composed of GPS-RTK, specially-made measuring rod, circular bubble, screws, cover and matching measuring cement pile. The function of each part is: the GPS-RTK obtain plane coordinate of measurement points. Specially-made measuring rod is made of invar material, can stretch and not affected by water and temperature, the height data of water surface can be directly read from the millimeter scale. The circular bubble can make sure the measuring rod stay in a vertical state. Screws are used for fixing the measuring rod and the cover. The cover is made of iron strip, avoiding the influence of water buoyancy and debris. The cement pile can closely combine with the cover.

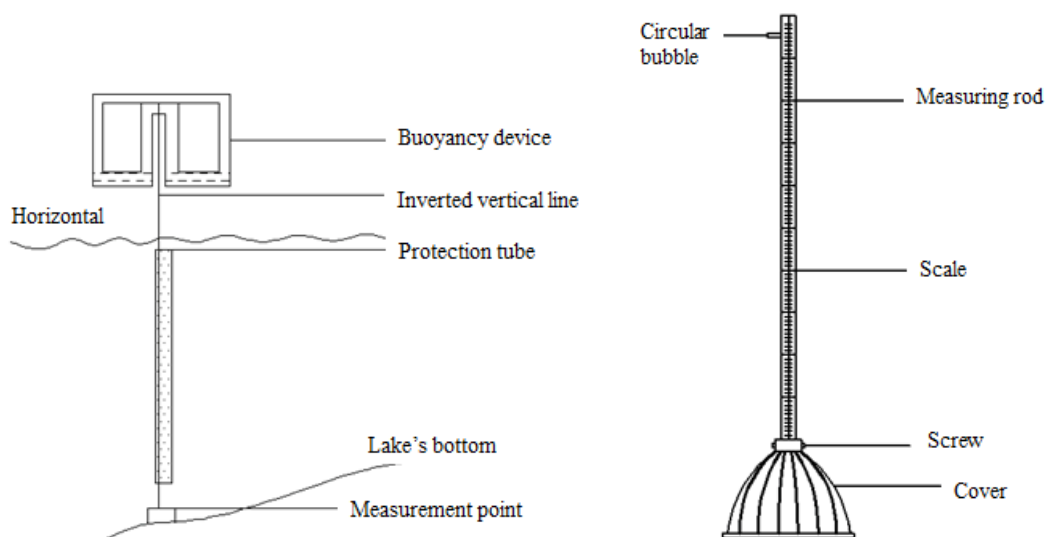


**Figure 1:** Inverted vertical rock movement measurement device

**Figure 2:** Specially-made measuring rod structure

### The 3D coordinates method of “Inverted vertical line measuring points method”

If there is no CORS station in the mine area, GPS base-station should be erected on the stable embankment near the lake, and RTK is carried on a ship for dynamic measurement. The ship carrying the RTK travels along the designed measurement route. When traveling to the inverted vertical line measuring points, RTK is placed on the tank of the buoyancy device after the float is stationary. After centering inverted vertical line, the coordinate  $(X_i, Y_i, Z_i)$  of the measurement point can be obtained. The method of elevation measurement is shown in Fig.3,  $D_i$  is the distance between the top of the inverted vertical line and the measurement point,  $S$  is the vertical distance between GPS receiver and the top of inverted vertical line (usually as a fixed value). Then the elevation of the measurement point  $i$  is:

$$H_i = Z_i - S - D_i$$

### The 3D coordinates measuring method of “the underwater measuring points with specially-made measuring rod method”

Similar to the last method, the GPS-RTK base-station is set up on embankment or island of the Weishan lake. The ship carrying the RTK travels along the designed measurement route. When traveling to the measurement point, RTK is placed directly on the measuring rod, and coordinate  $(X_i, Y_i, Z_i)$  of the measurement point can be measured. As shown in Fig.4,  $A_i$  (usually a fixed value) is the height from the top of rod to RTK,  $B_i$  is the length of measuring rod which adjusted to an appropriate length according to the water depth,  $K$  is a constant represents the distance between zero scale and the bottom of cover. Then the elevation of the measurement point  $i$  is:

$$H_i = Z_i - A_i - B_i - K$$

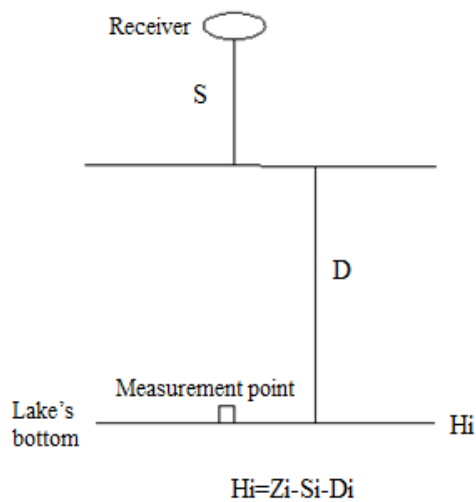


**Figure 3:** Height measurement method of "inverted vertical line measuring points method"

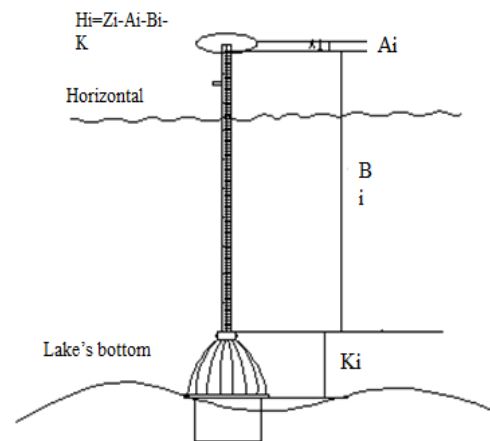


**Figure 4:** Working principle of specially-made measuring rod

## ANALYSIS OF MEASUREMENT ACCURACY

### Accuracy of plane measurement

In order to verify the plane accuracy of GPS-RTK, GPS-RTK and GPS static measurement experiments are carried out by use of two Tianbao 5800 GPS receivers and two Tianbao R4 GPS receivers in a coal mine of Shandong province in January 2015. The following conclusions can be found through the comparative analysis of these two sets of data: the plane error of measuring points is about 0.001m-0.012m when the distance between measuring points and base station is within 2km.

The relationship between the GPS-RTK plane measurement error and the distance from base station to mobile station is further analyzed by using weighted least squares method, as shown in Fig.5. The fitting function is follows and the error is 0.3.

$$y_3 = -1.57 \times 10^{-12} x^3 - 1.29 \times 10^{-8} x^2 - 2.39 \times 10^{-5} x + 0.017$$

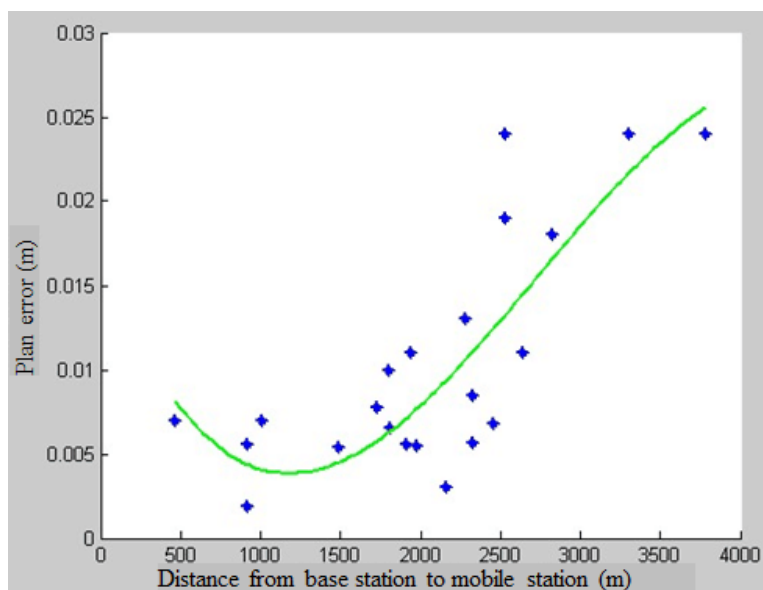


**Figure 5:** The fitting function image by weighted least squares

### Accuracy of elevation measurement

In order to verify the elevation accuracy of GPS-RTK, GPS-RTK elevation measurement and fourth-order leveling are carried out in a coal mine of Shandong province in February 2015. The following conclusions can be found through the comparative analysis of these two sets of elevation data: the error is about 0.002~0.096m when the distance from base station to mobile station is within 1km; the error is about 0.002~0.18m when the distance from base station to mobile station is within 1.5km; the error is about 0.002~0.282m when the distance from base station to mobile station is within 3km. The overall trend is: the farther the distance, the greater the error.

The relationship between the GPS-RTK elevation measurement error and the distance is further analyzed by using weighted least squares method, as shown in Fig.6. The fitting function is follows and the error is 0.04.

$$y_3 = -2.66 \times 10^{-8} x^2 + 0.00019x - 0.0054$$

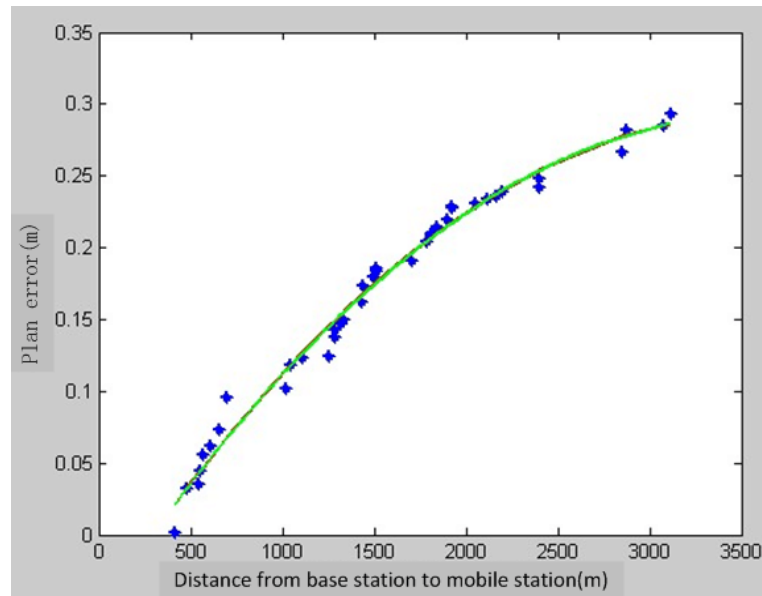


**Figure 6:** The fitting function image by weighted least squares

## ENGINEERING EXAMPLE

### Layout of observation stations and data collection

For a coal mine of Shandong province, the coal under the Weishan lake accounted for 2/3 of total coal reserves. The terrain in the lake's area is flat, with an average water depth of 1.8m. Underwater rock movement measurement is carried out in this lake area through two methods mentioned above. The deformation measurement began in March 2015 to the end of July 2016. As shown in Fig.7, two strike lines and four tendency lines are laid out respectively along the main section of coal seam strike and tendency. Based on the estimated results of probability integral method, in the area that the water depth is greater than 2m, the measuring points are laid according to "the inverted vertical line measuring points method"; in the area that the water depth is less than 2m, the measuring points are laid according to "the underwater measuring points with specially-made measuring rod method".

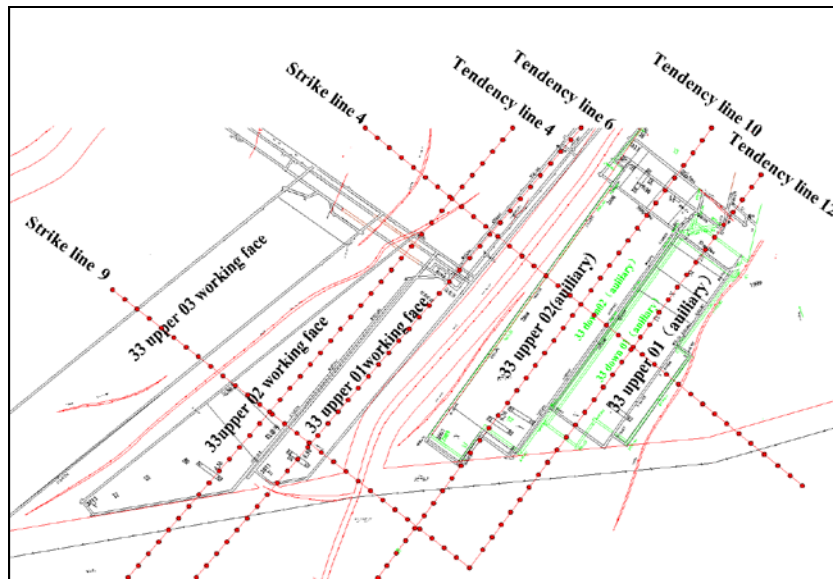


**Figure 7:** The layout diagram of main sectional plane measurement line

## Data processing and determination of rock displacement parameters

The subsidence curves of each strike line and tendency line are drawn by using “the mine surface determination forecasting and visualization system software”. Fig.8 is show the dynamic subsidence curves of strike line 9, boundary angles and displacement angles are indicated. Fig.9 is show the three-dimensional map of lake bottom deformation, and the rock movement coefficient as shown in Table 1.

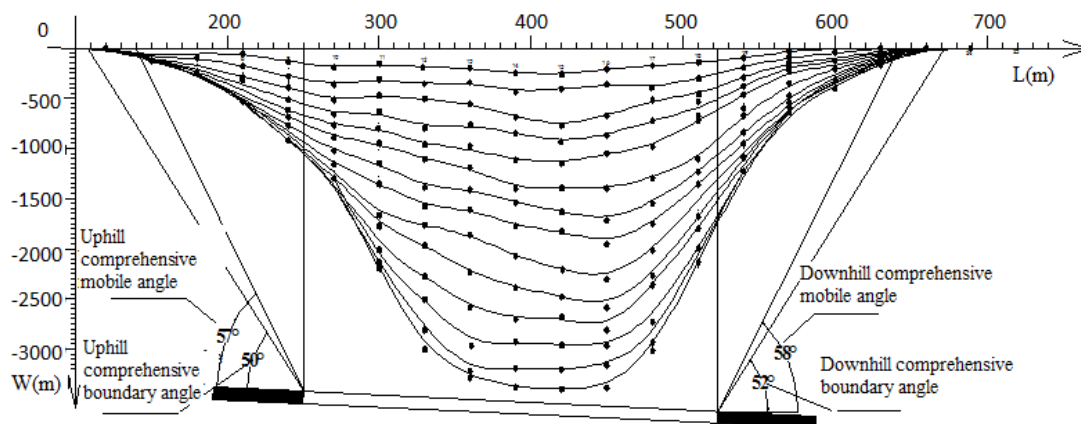


**Figure 8:** Dynamic subsidence curves of strike line 9

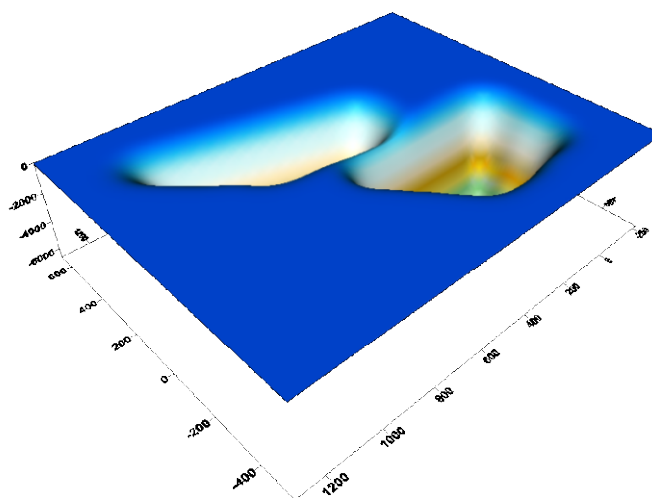


**Figure 9:** Three-dimensional map of Lake bottom deformation

**Table 1:** Rock movement coefficient

| Subsidence coefficient | Horizontal movement coefficient | $tg\beta$ | The greatest subsidence angle | Lithological coefficient |
|------------------------|---------------------------------|-----------|-------------------------------|--------------------------|
| 0.82                   | 0.28                            | 1.7       | $86^\circ$                    | 0.3                      |

## DEFORMATION PREDICTION OF THE METABOLIC GM (1,1)

### The metabolic GM (1,1)

As the commonly used grey model, the GM (1, 1) model includes the real-time model and the equal dimension real-time model. A real-time model is a model that adds each new information to the original sequence, then using the new sequence (Full sequence) to create a new model. The equal dimension real-time model is modeled by adding new information and removing old information at the same time, also known as the metabolic model<sup>[18]</sup>. The original data time sequence as follows:

$X^{(0)} = [x^{(0)}(1), x^{(0)}(2), \dots, x^{(0)}(n)]$ , and the new data time sequence

$X^{(1)} = [x^{(1)}(1), x^{(1)}(2), \dots, x^{(1)}(n)]$  is obtained through AGO, the formula is

( $k=1, 2, \dots, n$ ), and the GM (1, 1) is:

$$X^{(1)}(k+1) = \left[ X^{(0)}(1) - \frac{b}{a} \right] e^{-ak} + \frac{b}{a}$$

The a and b is called as grey parameters, which obtained by using the least square method and matlab fitting method, the formula is:

$$\hat{a} = (B^T B)^{-1} B^T Y = [a, b]^T$$

The cumulative matrix B and the constant vector Y are expressed as follows:



$$B = \begin{bmatrix} -\frac{1}{2}(x^{(1)}(1) + x^{(1)}(2)) & 1 \\ -\frac{1}{2}(x^{(1)}(2) + x^{(1)}(3)) & 1 \\ \vdots & \vdots \\ -\frac{1}{2}(x^{(1)}(n-1) + x^{(1)}(n)) & 1 \end{bmatrix}, Y = \begin{bmatrix} X^{(0)}(2) \\ X^{(0)}(3) \\ \dots \\ X^{(0)}(n) \end{bmatrix}$$

### The metabolic GM (1,1) prediction of point Z15 on strike line 9

Taking the measurement point Z15 on the strike line 9 as an example, the metabolic GM (1,1) modeling is carried out. The elevation values of Z15 are shown in Table 2.

**Table2:** The settlement measurement data table

| Serial number    | No. 1  | No.2   | No.3   | No.4   | No.5   |
|------------------|--------|--------|--------|--------|--------|
| Elevation values | 39.251 | 38.989 | 38.841 | 38.313 | 38.250 |
| Serial number    | No.6   | No.7   | No.8   | No.9   | No.10  |
| Elevation values | 38.101 | 37.861 | 37.626 | 37.429 | 37.035 |
| Serial number    | No.11  | No.12  | No.13  | No.14  | No.15  |
| Elevation values | 36.774 | 36.572 | 36.293 | 36.036 | 35.841 |

According to the metabolic GM (1, 1) modeling step, the dimension of the 15 subsidence data is chosen to be 4 ~ 15 (the dimension of the model is at least 4). The fitting accuracy test is shown in Table 3 and Table 4(in the unit of m).

**Table 3:** Model residual errors

| Dimension | 4    | 5    | 6    | 7     | 8     | 9     | 10   | 11   | 12   | 13   | 14   | 15   |
|-----------|------|------|------|-------|-------|-------|------|------|------|------|------|------|
| No.4      | 0.06 |      |      |       |       |       |      |      |      |      |      |      |
| No.5      | 0.26 | 0.08 |      |       |       |       |      |      |      |      |      |      |
| No.6      | 0.14 | 0.13 | 0.05 |       |       |       |      |      |      |      |      |      |
| No.7      | 0.16 | 0.02 | 0.04 | 0.02  |       |       |      |      |      |      |      |      |
| No.8      | 0.02 | 0.13 | 0.01 | 0     | 0.002 |       |      |      |      |      |      |      |
| No.9      | 0.04 | 0.03 | 0.07 | 0.01  | 0.025 | 0.15  |      |      |      |      |      |      |
| No.10     | 0.17 | 0.16 | 0.10 | 0.24  | 0.17  | 0.16  | 0.10 |      |      |      |      |      |
| No.11     | 0    | 0.05 | 0.07 | 0.10  | 0.18  | 0.14  | 0.14 | 0.10 |      |      |      |      |
| No.12     | 0.14 | 0.08 | 0.04 | 0.02  | 0.005 | 0.08  | 0.08 | 0.07 | 0.04 |      |      |      |
| No.13     | 0.04 | 0.04 | 0.03 | 0.007 | 0.01  | 0.03  | 0.1  | 0.09 | 0.09 | 0.07 |      |      |
| No.14     | 0.03 | 0.03 | 0.03 | 0.02  | 0.007 | 0.007 | 0.03 | 0.09 | 0.08 | 0.09 | 0.07 |      |
| No.15     | 0.07 | 0.04 | 0.04 | 0.08  | 0.08  | 0.07  | 0.06 | 0.05 | 0.04 | 0.04 | 0.03 | 0.02 |

**Table 4:** Mean errors of model residual

| Dimension                         | 4    | 5    | 6    | 7    | 8    | 9    | 10   | 11   | 12   | 13   | 14   | 15   |
|-----------------------------------|------|------|------|------|------|------|------|------|------|------|------|------|
| Mean errors of model residual (m) | 0.11 | 0.08 | 0.05 | 0.09 | 0.09 | 0.11 | 0.09 | 0.08 | 0.07 | 0.07 | 0.05 | 0.02 |

It can be seen from Table 3 and Table 4 that when the dimension is increasing, the prediction accuracy is not improved linearly, but reduced. This means that the metabolic GM ( 1,1) has the best dimension region, and the dimension is not the more the better.

When the dimension is 6, the predicted results are relatively good and the prediction accuracy is the highest, which can be used to monitor and forecast. So the best model dimension is 6. The posterior-variance-test shows that the accuracy grade of the model is grade 1.

The comparison between the measured value and the predicted value is shown in Table 5 and Fig.10. It is obvious that the metabolic GM (1,1) model is more accurate than the ordinary GM (1,1).

**Table 5:** Comparison of the measured values and the predicted values for Z15

| Serial number | Measured value (m) | Prediction of the metabolic GM ( 1,1) |              | Prediction of the ordinary GM ( 1,1) |              |
|---------------|--------------------|---------------------------------------|--------------|--------------------------------------|--------------|
|               |                    | Predicted values (m)                  | Residual (m) | Predicted values (m)                 | Residual (m) |
| No.1          | 0                  | 0                                     | 0            | 0                                    | 0            |
| No.2          | -0.262             | -0.277                                | 0.015        | -0.277                               | 0.015        |
| No.3          | -0.410             | -0.51                                 | 0.100        | -0.516                               | 0.106        |
| No.4          | -0.938             | -0.742                                | -0.196       | -0.742                               | -0.196       |
| No.5          | -0.999             | -0.99                                 | -0.009       | -0.99                                | -0.009       |
| No.6          | -1.150             | -1.200                                | 0.05         | -1.224                               | 0.074        |
| No.7          | -1.39              | -1.430                                | 0.04         | -1.456                               | 0.066        |
| No.8          | -1.625             | -1.615                                | -0.01        | -1.686                               | 0.061        |
| No.9          | -1.822             | -1.752                                | -0.07        | -1.914                               | 0.092        |
| No.10         | -2.216             | -2.116                                | -0.1         | -2.141                               | -0.075       |
| No.11         | -2.477             | -2.407                                | -0.07        | -2.365                               | -0.112       |
| No.12         | -2.679             | -2.719                                | 0.04         | -2.588                               | -0.091       |
| No.13         | -2.958             | -2.988                                | 0.03         | -2.808                               | -0.15        |
| No.14         | -3.215             | -3.245                                | 0.03         | -3.027                               | -0.188       |
| No.15         | -3.410             | -3.450                                | 0.04         | -3.155                               | -0.255       |

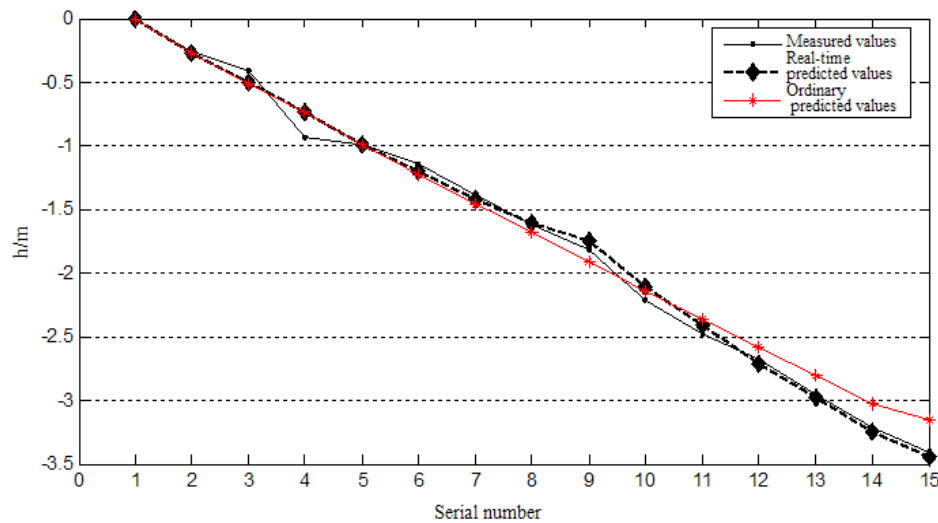


**Figure 10:** Comparison of measured values and predicted values for Z15

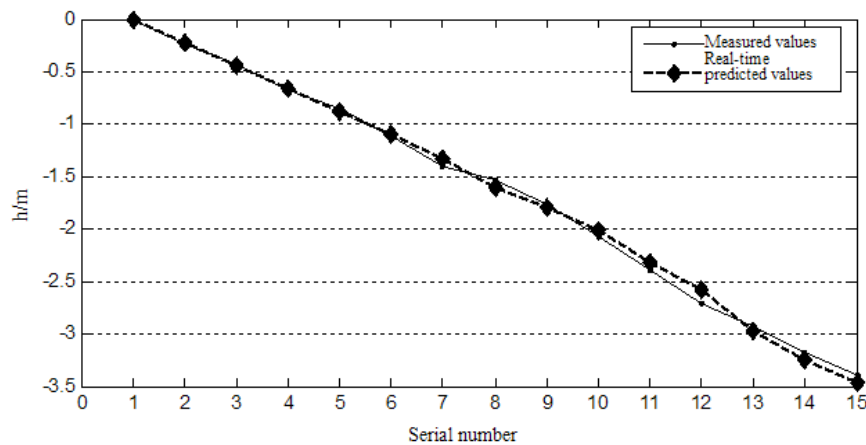
### The metabolic GM (1,1) prediction of point Z14, Z13 and Z12 on strike line 9

Similarly, the metabolic GM (1,1) prediction of points Z14, Z13 and Z12 on the line 9 is carried out. The fitting accuracy is shown in Table 6 (the unit is m).

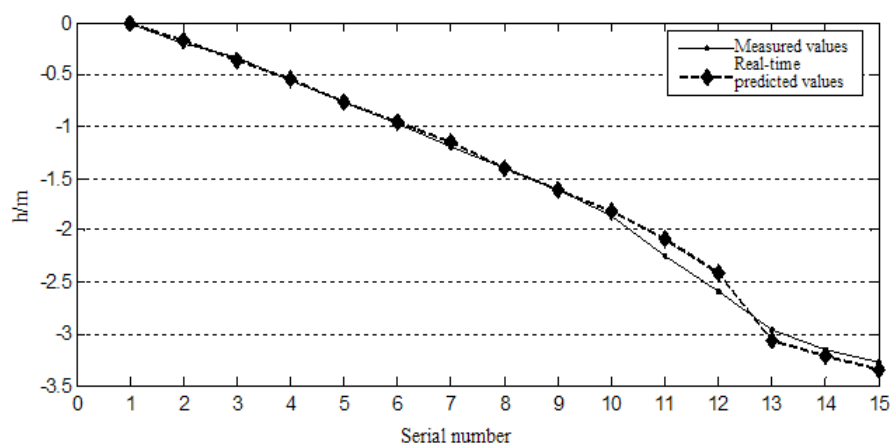
**Table 6:** Mean errors of model residual

| Dimension | 4    | 5    | 6    | 7    | 8    | 9    | 10   | 11   | 12   | 13   | 14   | 15   |
|-----------|------|------|------|------|------|------|------|------|------|------|------|------|
| Z14       | 0.09 | 0.08 | 0.06 | 0.09 | 0.08 | 0.10 | 0.12 | 0.08 | 0.08 | 0.07 | 0.07 | 0.03 |
| Z13       | 0.10 | 0.09 | 0.07 | 0.09 | 0.09 | 0.11 | 0.09 | 0.08 | 0.08 | 0.08 | 0.09 | 0.03 |
| Z12       | 0.08 | 0.08 | 0.05 | 0.10 | 0.09 | 0.08 | 0.07 | 0.08 | 0.07 | 0.07 | 0.10 | 0.04 |

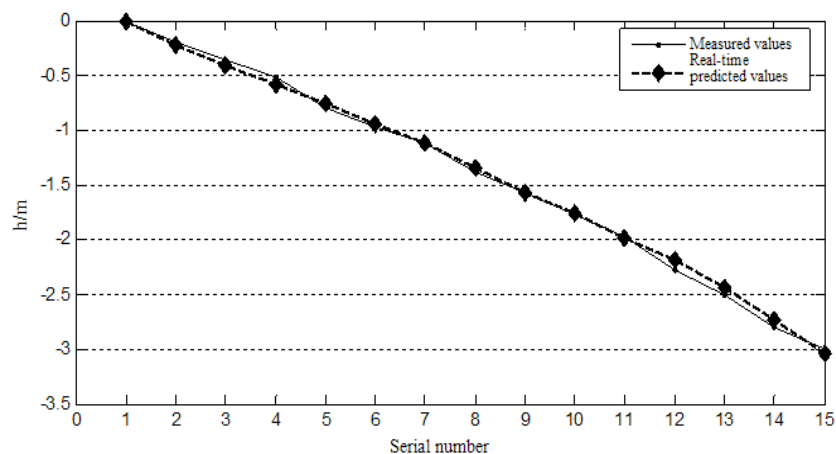
Through the comparison of accuracy, the most suitable dimension of the model is 6. The metabolic GM (1, 1) of these three points was established, and the comparison between the measured values and the predicted values are shown in Fig. 11.



(a) point Z14



(b) point Z13



(c) point Z12

**Figure 11:** Comparison of measured values and predicted values

## Evaluating the accuracy grade of the model

According to the posterior-variance-test, the accuracy of the prediction model is evaluated synthetically through posterior difference ratio  $C$  and small error probability  $P$ . The prediction accuracy grade of the four points Z15, Z14, Z13 and Z12 on line 9 is grade 1, the accuracy is high.

## CONCLUSIONS

"The inverted vertical line measuring points method" and "the underwater measuring points with specially-made measuring rod method" are designed respectively to solve the problems of coal mining in deep and shallow water. The feasibility of the aboved methods are proved by practical application, which provides a new and reliable method for deformation measurement under the still water.

In order to verify the accuracy of GPS-RTK, GPS static measurement experiments and fourth-order leveling are carried out, and the measurement results are compared with GPS-RTK data. The

function relationship between the GPS-RTK measurement error and the distance from mobile station to base station is identified.

This method is applied to lake-bottom deformation measurement. The three-dimensional deformation map and subsidence curves of the measurement lines on the main section are drawn, and the rock movement parameters are obtained.

Based on the gray theory, the six-dimensional metabolic GM (1,1) are established for the deformation monitoring points Z15, Z14, Z13 and Z12 on strike line 9. The average residual values are 0.05m, 0.06m, 0.07m and 0.05m, and the accuracy grade of the model are grade 1. The metabolic GM (1,1) can not only reflect the dynamic changes of the measurement points over time, but also highlight the latest trends of future disturbance factor entry into the project, with engineering practical value.

## REFERENCES

- [1] XIAO Haiping, CHEN Lanlan. Application of grey theory model in monitoring mine deformation[J]. *Metal Mine*, 2009(1):154-155
- [2] JIANG Lishuai, Sainoki A, Mitri H S, et al. Influence of fracture-induced weakening on coal mine gateroad stability[J]. *International Journal of Rock Mechanics & Mining Sciences*, 2016, 88:307-317.
- [3] WANG Youliang, TANG Yuegang. Curve fitting and GM(1,1) model subsidence forecast and relevant analysis[J]. *Science of Surveying and Mapping*, 2008,03:98-99+78
- [4] LIU Hechun, GUO Qiu. Prediction of the mining subsidence of xihaozhuang iron mine based on GPStechinque and Grey model [J]. *Metal Mine*, 2016(10)
- [5] SONG Shijie, ZHAO Xiaoguang, LIU Yuan. Grey relational analysis and regression forecast of Yushenfu mining subsidence [J]. *Safety in Coal Mines*, 2010,41(8):138-140
- [6] YANG Junkai, Fan Hongdong, Zhao Weiyong. Monitoring and prediction of mining subsidence based onD-In SAR and Gray verhulst model[J]. *Metal Mine*, 2015,44(3):143-147
- [7] HOU Cunlai, WU Aixiang, WANG Yiming. Control and prediction on surface subsidence for mining under highway[J]. *Mining R&D*, 2016(5)
- [8] FEI Zhang, Aibing Ge, Fei Li, and Guangjun Shen: “Deformation and Stability Problems in Large, Deep, Near -River Excavations—A Case Study” *Electronic Journal of Geotechnical Engineering*, 2016 (21.21), pp 6745- 6753.
- [9] BO Hailong, Wang Lijuan, Zhou Xiaoping. Numerical analysis of ground settlement in mining areas under the railway[J]. *Traffic engineering and technology for national deffence*, 2009, 7(1):29-30
- [10] ZHE H, YI Z, CHAO H. Mechanical mechanism of water inrush in the side of karst tunnel under the effect of fault[J]. *Electronic Journal of Geotechnical Engineering*, 2014, 19:4611-4622.

- [11] YIN Haifeng. Application research of the GPS on underwater topographic survey[D]. Tsinghua University, 2008
- [12] Wang Y, Bai H, Chen Y, et al. Development law of water flowing fractured zone in the thin bedrock area of Sima mine[J]. *Electronic Journal of Geotechnical Engineering*, 2014, 19:5715-5724.
- [13] JIN Yingchao, CHEN Ming. Application of GPS-RTK cooperating with depth sounder in huangbizhuang reservoir underwater survey[J]. *Water Sciences and Engineering Technology*, 2005,(4)
- [14] YANG Fan, XU Jian, XU Weidong, Application of real-time kinematic technology to shipping lane survey [J]. *Bulletin of Surveying and Mapping*, 2001,(2)
- [15] LI Dongsheng, HUANG Teng, LIU Weidong, et al. Application of GPS RTK to Islands Survey [J]. *Modern Surveying and Mapping*. 2011,(4)
- [16] ZHOU Jianzheng, YANG Zhongli. Application of GPS real-time dynamic measurement of underwater topographic survey in Guxian Reservoir[J]. *Hydrographic Surveying and Charting*, 2002, (3)
- [17] BAN Xunhai, LI Jingtao, LUAN Yuanzhong, et al. Analysis of GPS-RTK observation data in subsidence of Weishan lake[J]. *Mine Surveying*, 2010,(4):11-13
- [18] DENG Julong. Grey theory foundation [M].Wu Han: Huazhong University of Science & Technology Press. 2003



© 2017 ejge

***Editor's note.***

This paper may be referred to, in other articles, as:

Yuanzhong Luan, Liyuan Weng, Yanhe Ma, and Hengxuan Luan: "Lake-Bottom Deformation Special Equipment Measurement Methods and Practice of Mining Under Weishan Lake" *Electronic Journal of Geotechnical Engineering*, 2017 (22.04), pp 1363-1376. Available at [ejge.com](http://ejge.com).